Natural Resources for Human Health
eISSN: 2583-1194

Original Research

Received 18 May 2026
Revised 29 June 2026
Accepted 16 July 2026

Natural Resources for Human Health 2026, Vol. 6(8s): 1511–1524

KEYWORDS:
Perovskite solar cells, Lead-free perovskites, Optical modelling, Lead-based perovskites, Carrier generation.

Comparative Analysis of Lead-Based and Lead-Free Perovskite Solar Cells

Sunaina[1], Pardeep Kumar[2*], Ashish Grover[3*]

[1] Research Scholar, Department of Applied Sciences (Physics), School of Engineering and Technology, Manav Rachna International Institute of Research and Studies (MRIIRS), Faridabad, Haryana, India
Email: 1bsunaina@gmail.com
[2] Professor, Department of Applied Sciences (Physics), School of Engineering and Technology, Manav Rachna, International Institute of Research and Studies (MRIIRS), Faridabad, Haryana, India, Email: pvc.pk@mriu.edu.in
[3] Professor, Department of Applied Sciences (Physics), School of Engineering and Technology, Manav Rachna, International Institute of Research and Studies (MRIIRS), Faridabad, Haryana, India, Email: ashishgrover.set@mriu.edu.in

ABSTRACT: The current study provides a comparative report on lead-based and lead-free perovskite solar cells with emphasis on efficiency, stability and dependability of operation. There are two approaches to modeling. A coupled optical-electrical model is used to study the lead-free perovskite solar cell, whereas a numerical optical model is used to study lead based materials under the same illumination conditions. The findings indicate that the lead-free perovskite ($Cs_2AgBiBr_6$) can be able to attain a maximum simulated efficiency of approximately 21% in an optimal thickness of 75 nm. But the electrical performance is very low with the current density of approximately 0.026 mA/cm² and efficiency of only 0.00051% in the actual conditions. Contrary to this, lead-based compounds like $FAPbI_3$ and $MAPbI_3$ can be optically absorbed to 850 nm or higher with much higher ideal current densities with $FAPbI_3$ absorbing to 1.15×10^{-13} mA/cm². Carrier generation and deep penetration of the light is equally better in lead/based materials. There are however toxicity and stability problems with them. The research proves that there is a definite trade-off between high efficiency and environmental safety and therefore more studies are required in an effort of ensuring better lead-free material can be used practically.

1. INTRODUCTION

Perovskite solar cells are an emerging relevant technology because of the high efficiency and low cost of the product. $MAPbI_3$ and $FAPbI_3$ are some of the perovskites based on lead have demonstrated a great performance in terms of high-power conversion efficiency and intense light absorption. The fact that there is lead poses severe environmental and health-related problems. This has seen an interest in lead-free perovskite $Cs_2AgBiBr_6$, $MASnI_3$, and bismuth-based and tin-based perovskites increase. Even though safe and more stable materials where lead-free, these materials tend to demonstrate poorer efficiency and poor electrical performances. This brings about a necessity of comparison in great details between lead-based and lead-free systems. The present paper provides an analysis of both kinds of materials in respect to various modeling approaches. This is aimed at comparing their optical behavior, carrier generation and performance of the devices. The research assisted in comprehending the weaknesses and strengths of every system and gives future research directions.

A number of researchers have delved into the mechanics of lead-free perovskite solar cells (PSCs). Al Atem et al. (2025) [1] employed SCAPS-1D simulations in their work designing Sn-based and Ge-based PSCs, which Sn-based devices oriented at a record of 23.19% power conversion efficiency (PCE). In a notable study, Bhattarai et al. (2022) [15] presented the graded absorber layer concept using $MASnI_3$ material and achieved power conversion efficiency (PCE) of 22.3% with the proper

absorber thickness, defect density, and back contact materials optimization. Ali et al. (2025) [13] employed simulations for $CsBi_3I_{10}$-based PSCs for and optimized the electron and hole transport layers for power conversion efficiency (PCE) of 11.98%. Donkata et al. (2025) [19] used a combined approach of DFT and drift-diffusion modeling to simulate a fully inorganic heterojunction cell ($FTO/WS_2/CsBaCl_3/rGO/Pt$) reaching a theoretical output power of 33% and proved the possibility of forming new stable lead-free architectures. Together, all the proposed studies display the immense possibility of lead-free PSCs that can harmoniously compete with lead counterparts, by identifying new design strategies and methodologies for optimizations. Aside from solar cells, lead-free perovskites have been promising other optoelectronic devices. Zhang et al. (2024) [15] summarized lead-free metal halides for resistive memories and artificial synapses with respect to switching mechanisms and fabrication methods while delineating challenges to future work. Rahimi et al. (2024) [19] enhanced light extraction efficiency by a factor of ten for LEDs based on perovskites using a domical structure with up to 74% LEE. Sulaman et al. (2022) [8] utilized surface passivation by P3HT on $CsSnBr_3$ photodetectors to increase responsivity to 1.56 A/W and detectivity to 1.40×10^{14} Jones. Yan et al. (2022) [20] investigated the effects of ion migration in $CsCu_2I_3$ single-crystal microrod photodetectors, exhibiting higher on/off ratios and better stability. Finally, Salem et al. (2025) [8] performed TCAD simulations for the design of $AgBiI_4$-based indoor photovoltaics for IoT devices with enhanced module efficiency from 5.15% to 23.58% under LED light conditions.

The optimization of perovskite absorber layers by experimental methods, although inevitable, could be time-consuming and expensive, and highly susceptible to processing variabilities [16] Many rounds of fabrication and analysis are necessary in order to estimate the effects of layer thickness, composition, and interfaces on device performance [17]. Under these circumstances, numerical optical modeling has proved to be an important and useful aid to experimental work [4]. Using numerical solutions to Maxwell's equations with suitable boundary conditions, numerical optical models are capable of simulating light transport, absorption, and optical losses in multilayer solar cell structures [14]. Numerical optical modeling allows physical understanding of optical processes that are difficult to identify experimentally. Numerical optical modeling makes it possible to assess systematically the properties of the absorber layer without being limited by material availability or fabrication constraints [18]. Simulations allow the study of some key optical parameters like absorption, reflectance, transmittance, and optical generation rate these can be studied as functions of the absorber thickness and material constants [11]. With this method, one can find optimal thickness ranges for maximum photon absorption with minimal recombination and parasitic losses [7]. Optical modeling helps understand interference effects due to multiple reflections at the interfaces between transparent conductive oxides, transport layers, and metallic back contacts; these are particularly important in thin-film perovskite devices [12].

Another important advantage of numerical optical modeling is that it may serve to evaluate various design strategies for light management [3]. Various techniques, including refractive index engineering, anti-reflection coatings, textured interfaces, and graded absorber layers, can be virtually tested before experimental implementation [10]. Provided that these strategies ensure an optimization of optical confinement and enhance the effective optical path length within the perovskite absorber, this can result in a significant improvement of short-circuit current density and device efficiency generally [5]. Numerical modeling offers a route for comparing various perovskite compositions and bandgap values under standard solar illumination, supporting the development of both single-junction and tandem solar cell configurations.

2. METHODOLOGY

2.1 Comparative Modeling Framework

This study has a comparative framework as its methodology since it compares the performance of lead-free and lead-based perovskite solar cells under an identical optical environment. The key objective is to evaluate their performance based on efficiency, stability as well as operational dependability. There are two models employed. In the case of lead-free perovskites, a coupled optical electrical model is utilized whereas in the case of lead-based perovskites a simplified numerical optical model is employed.

The two models assume the occurrence of light interactions with an absorber covering on the wavelength range of 300 nm to 900 nm. The useful solar spectrum is mostly enclosed in this range which includes the ultraviolet, visible and near-infrared regions. In both cases, the same illumination condition, as in AM1.5G standard, is used to be able to fairly compare the cases. Each perovskite system has material characteristics including thickness, absorption coefficient and even wavelength-dependent characteristics. The major difference between the two models is that, in the lead-free model, the two processes are combined in the optical and electrical processes and the lead-based model only considers the optical absorption with ideal carrier

generation processes. This disparity is significant in the context of the knowledge of the disconnect between the theoretical and practical performance.

2.2 Optical Modeling and Carrier Generation

The two systems are studied to determine the optical behavior which investigates the absorption of light and conversion to a charge carrier. In the case of lead-free perovskites, the reflection, transmission and absorption in a multi-layer devices structure is computed by means of the Transfer Matrix Method (TMM). The approach takes into account interference effects and field distribution of optical fields within each of the layers.

In the case of lead-based perovskites, a simplified Beer-Lambert law is applied in order to obtain the absorption. This method presupposes that the intensity of light reduces exponentially as one goes deeper into the material. The relation is used to obtain the absorbance:

$$\mathbf{A(\lambda) = 1 - e^{-\alpha(\lambda)t}} \quad (1)$$

with α(λ) and t are the absorber layer thickness.

The energy of photons at each wavelength is:

$$\mathbf{E(\lambda) = \frac{hc}{\lambda}} \quad (2)$$

This assists in establishing the contribution of photons of various wavelengths towards the development of carriers.

It is estimated by calculating the density of the current of the short-circuit as the centre of the flux of the absorbed photons:

$$\mathbf{J_{sc} = q \int \Phi(\lambda) A(\lambda)\ d\lambda} \quad (3)$$

The assumptions in the lead model are that every absorbed photon creates one electron, that is, quantum efficiency is 100%. The current generation is given an optimum limit by this. Another model, the lead-free one, on the other hand, calculates depth-dependent carrier generation profiles using realistic optical inputs.

2.3 Electrical Modeling and Performance Evaluation

The electrical performance is offered as the case of the lead-free perovskite solar cell. Optical modeling is applied to create a generation profile, which is used as the input in the Diabolic equations of carrier transport. The movement of the electrons and holes inside in the device is investigated in a one-dimensional drift diffusion model.

The model has significant physical processes which are the recruiting of carriers, their movements, and diffusion. Calculation of the current voltage (J-V) properties is accomplished by subjecting it to varied voltage conditions. Based on this curve, some of the important areas of performance parameters are short-circuit current density, open-circuit voltage, fill factor and power conversion efficiency.

The productivity is estimated with the help of equation:

$$\mathbf{\eta = \frac{J_{sc} \times V_{oc} \times FF}{P_{in}}} \quad (4)$$

where P_{in} power of the incident sun.

Lead-free model has also an optimization procedure consisting of the variation of the absorber thickness. This assists in determining the level at which the machine is the most effective. In the lead-based case, electrical modeling is missing, which is a weakness, but it provides an opportunity to have a coherent comparison between a perfectly performing optical model and the real-world behavior of a device.

3. RESULTS AND COMPARATIVE ANALYSIS

3.1 Thickness Optimization and Efficiency Behavior (Lead-Free Focus)

The variation in device efficiency with absorber layer thickness reveals a clear dependence, with peak performance reaching approximately 21% at an optimal thickness of around 75 nm. This suggests the presence of an ideal thickness at which the device operates most efficiently. At lower thicknesses, the material is insufficient to absorb an adequate amount of incident light, thereby limiting charge carrier generation and reducing overall efficiency. Beyond the optimal level of thickness, carrier transport is still efficient and becomes light absorptive, and therefore, the performance is maximized. Figure 1 presents the trend in efficiency across different absorber layer thicknesses in a lead-free perovskite solar cell.

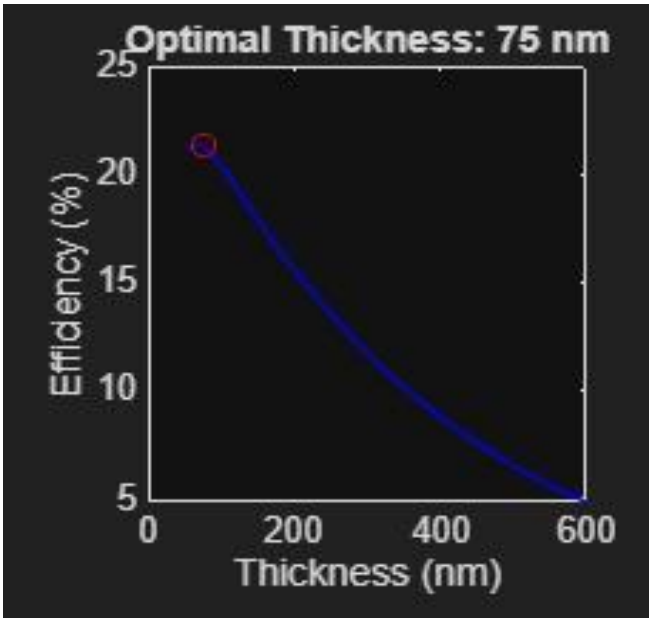

Figure 1: Optimal Thickness

At a thickness beyond this optimal, the efficiency approaches a constant with an increase in its thickness. This action is explicable on the basis of rises in recombination losses and transport restrictions. Photogenerated carriers have to go over a longer distance in plumper layers in order to reach the electrodes which heightens the chance of recombination prior to collection. Thus, although the optical absorption rises with the thickness, electrical losses is overwhelming and the total efficiency diminished. A major drawback of lead-free perovskite materials is emphasized in this outcome. They have carrier mobility and a diffusion length insufficient to support absorber layers of a greater thickness. As compared to these, the lead-based perovskites are reported to be able to sustain their high performance even at greater thicknesses because their transport characteristics are better and their recombination rates are reduced. Thus, though the simulation indicates that the theoretical efficiency will be high at the optimum thickness, there is less sensitivity to changes in thickness, which implies that lead-free systems will be less reliable in terms of operations.

3.2 Optical Properties Comparison (Absorption, Reflection, Transmission)

Figure 2 represents optical characteristics of lead-free perovskite material both in the absorption and the reflection spectrum between the wavelengths of 300 nm and 900 nm.

Natural Resources for Human Health
eISSN: 2583-1194

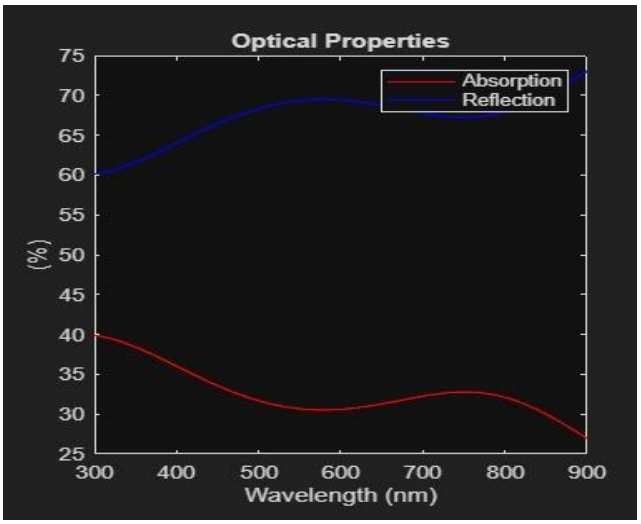

Figure 2: Optical Properties (Lead-Free)

The number shows a prevalence of reflection in most areas of the spectrum, which is up to 70 percent in the visible part of the spectrum. The level of absorption is comparatively low and reduces slowly with increase in wavelength. This decreasing relationship between the reflection and the absorption implies that a high proportion of incident light does not go to waste to generate the carriers. The loss of reflection is high and limits the overall effective photon flux that passes to the absorber layer and this affects the performance of the device. In the case of lead-based materials, Figure 3 demonstrates the spectral behavior of the absorbance of various perovskite absorbers.

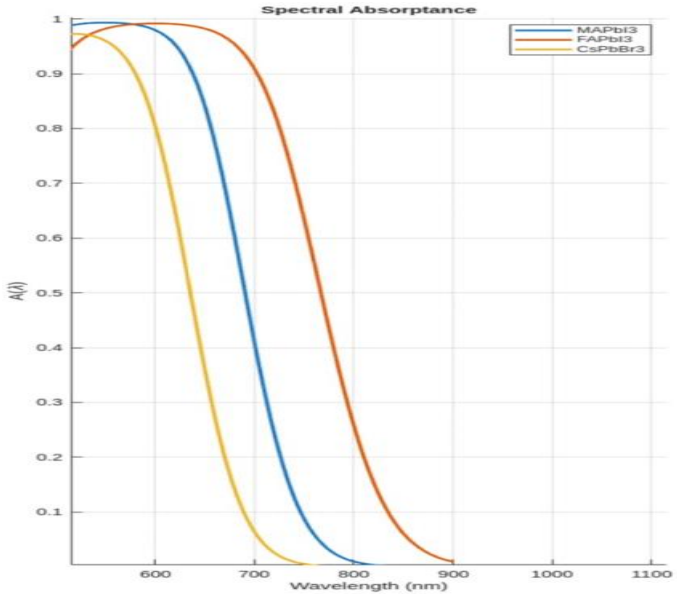

Figure 3: Spectral Absorbance (Lead-Based)

It has been shown through the absorbance curves that lead-based material is very strong and broadly absorbed in the visible and near-infrared regions. The $FAPbI_3$ demonstrates the widest range of absorption that goes as far as about 850 nm. This increased absorption enables it to pick up a larger size of the solar or the photons that are lower in power, which amplifies greatly the generation of the current. The values of the absorption coefficient are extremely large especially that of the $MAPbI_3$ meaning that the light and the material interact strongly. $FAPbI_3$ has a reduced peak but a more extended distribution, which is positive in collecting the light in a larger wavelength range (Figure 4). This tendency can be explained by the impact of bandgap tuning caused by the material composition that is one of the primary strengths of lead-based perovskites.

Natural Resources for Human Health
eISSN: 2583-1194

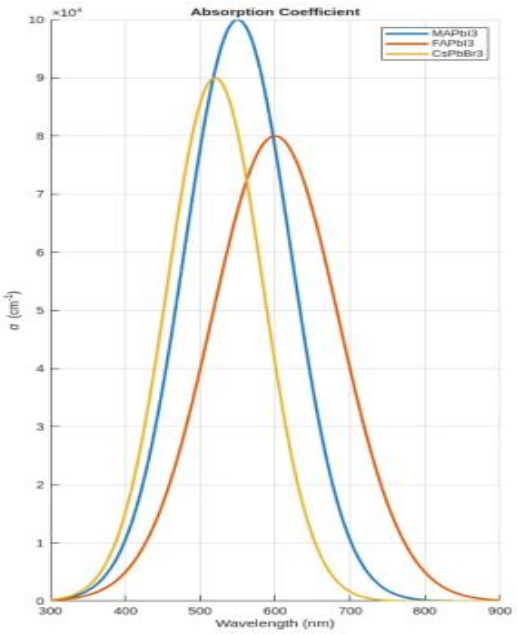

Figure 4: Absorptiometry of Lead based Materials

The reflection is very low and is almost unchanged with all wavelengths. This is an indication that the incident light is reflected into the absorber layer and optical losses are minimized. This is also a major strength over the lead-free material, whereby there is a high reflection loss, which is extremely wavelength-dependent (Figure 5).

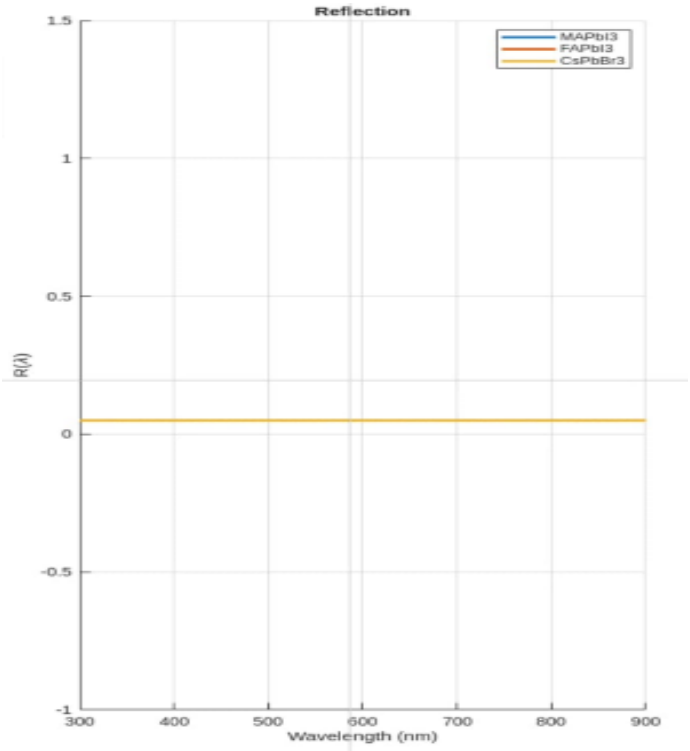

Figure 5: Reflection Characteristics of Lead based Materials

The transmission curves (Figure 6) indicate that materials made of lead absorb the greatest amount of light in the visible wavelength because the values of transmission are very low during the visible wavelength. The bandgap of every material is

believed to be the wavelength at which the transmission starts rising. $FAPbI_3$ reveals sluggish transmission recovery which confirms that it has the capability of taking up longer wavelengths.

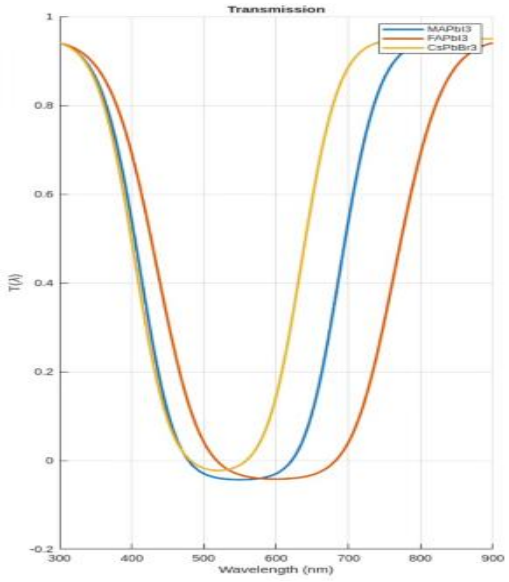

Figure 6: Transmission Characteristics

Based on the optical comparison, it is clear that Lead based perovskites are better light harvesting material because they have extended absorption; it has large absorption coefficients as well as low losses in terms of reflection. Meanwhile, lead free materials lack absorption, and as a result of this, the absorption is minimal and reflected a lot depicting inefficiency.

3.3 Spectral Response and Quantum Efficiency

The EQE curve indicates that the device is quite efficient in the short wavelengths with a close to 100% efficiency at the short wavelengths around 300 nm. It means that charge carriers are produced efficiently as a result of high-energy photons. The EQE however drops off very swiftly with a rise in wavelength and tends to zero at a wavelength of about 650 nm and above. This severe discontinuity implies that the material cannot absorb and make use of low-energy photons (Figure 7).

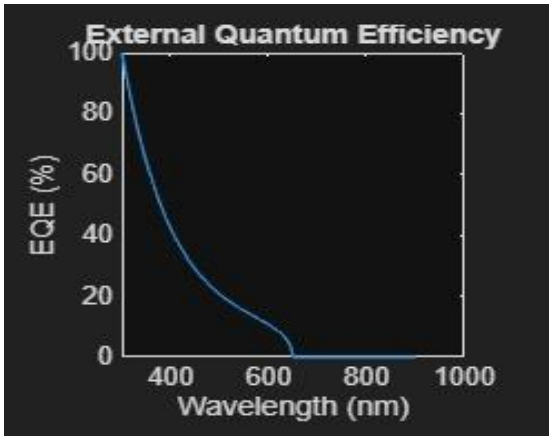

Figure 7: EQE of the lead-free perovskite solar cell.

This is directly associated to the bandgap of the material. The bigger band gap inhibits absorption of longer wavelengths thereby reducing the useful part of the solar spectrum. Consequently, the device is unable to produce enough current in red and near-infrared of the solar radiation which forms a substantive fraction of the total solar radiation.

In the case of the lead-based materials, the EQE data are not actually displayed in the presented results. Another characteristic of their absorption property would be, however, their broader spectral response. Countries such as $FAPbI_3$ that absorb up to

850 nm are most likely to record better values of EQE in a broader range of wavelengths. This suggests improved use of photons and maximized current production.

The lack of EQE data of lead-based materials is a weakness to the comparison, which is, however, overwhelmed by the optical data the lead-based materials showed. Spectral response wise, the lead-based perovskites are more efficient and be able to utilize a larger portion of the solar spectrum than the lead-free materials.

3.4 Carrier Generation Analysis

Figure 8 can be used to determine the profile of the generation of the lead-free perovskite versus depth and wavelength.

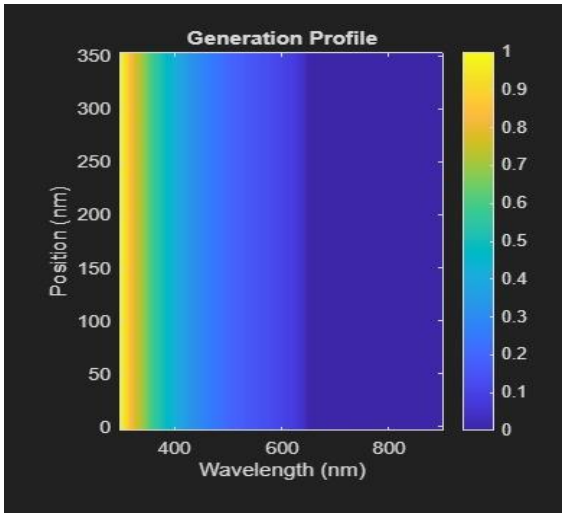

Figure 8: Generation Profile (Lead-Free)

The heat map shows that generation of carriers is in high concentrations by the surface and short wavelengths. The higher the depth the lower the rate of generation. This implies that the incidence query of the light is considerable towards the surface, and the quantity of light which passes further into the substance is minimal. Generation is insignificant at wavelengths above 600 nm, and this is again indicative of the limitation by bandgaps.

Figure 9 illustrates the rate of spectral generation of lead-based materials.

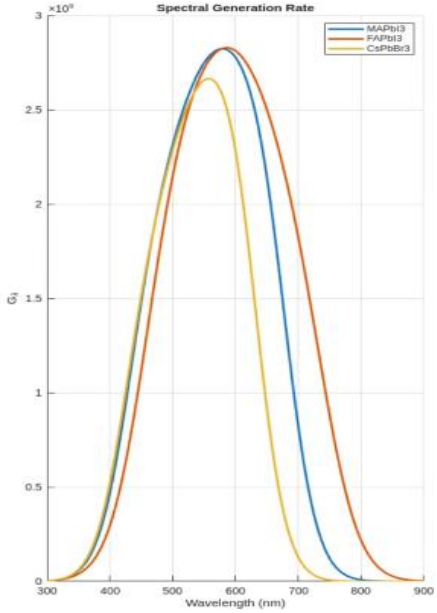

Figure 9: Spectral Generation Rate

The curve indicates that $FAPbI_3$ is the most generated substance of all wavelengths with a high-generation rate than $MAPbI_3$. $CsPbBr_3$ generates less since it has a larger bandgap. The extended generation range of $FAPbI_3$ means that the solar radiation is well taken advantage of.

Figure 10 is the cumulative carrier generation.

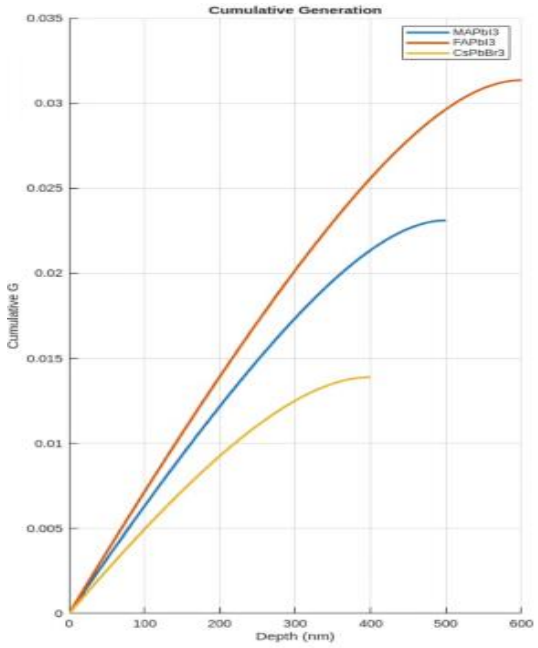

Figure 10: Cumulative Generation

This means that $FAPbI_3$ generates maximum number of carriers across the thickness of the material as shown in the cumulative generation curves. $MAPbI_3$ and $CsPbBr_3$ have moderate and low performance respectively. This is an amalgamation of range of absorption as well as of penetration.

Generation vs depth is represented in figure 11.

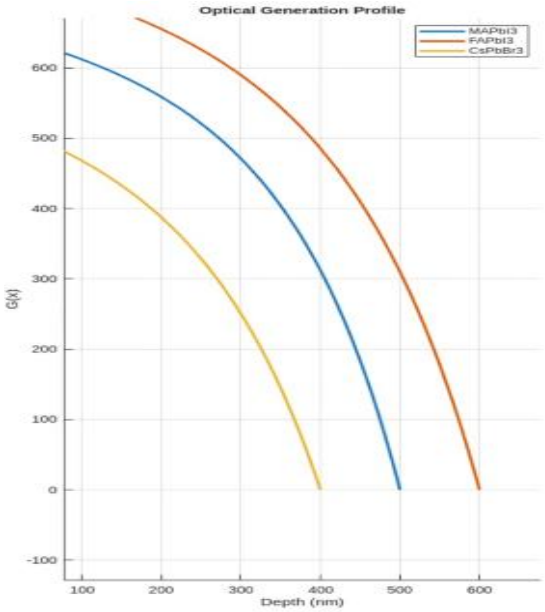

Figure 11: Generation vs Depth

The value shows that the lead-based materials permit the deeper penetration of the light and uneven generation throughout the thickness. Conversely, the materials that do not contain lead exhibit a high surface limited generation profile.

In this comparison, it is notable that unlike in the previous case of lead-based materials, they not only produce more carriers but also spread them better across the absorber layer. The skewed shape in carrier collection and higher recombination in generation that exists in lead-free materials has a detrimental effect on performance.

3.5 Electrical Performance and Carrier Transport

The J-V curve suggests that the performance of the device is quite poor with very low current density and voltage values. The curve is not of an expected shape of a rectangle that is characteristic of an efficient solar cell. Rather it exhibits almost linear like behavior which means it has high internal resistance and low extraction of charge. The J-V characteristics of the lead-free perovskite solar cell are presented in figure 12.

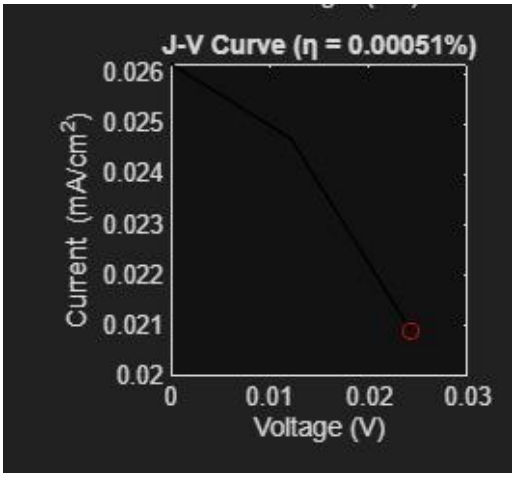

Figure 12: J–V Curve

The carrier distributions indicate that there was a distinct split of the electron and hole concentrations throughout the device. The point of intersection shows where recombination most probably can take place. The high gradients indicate that the transportation of carriers is not carried out efficiently resulting in high recombination losses. Profiles of the carrier concentration are presented in figure 13.

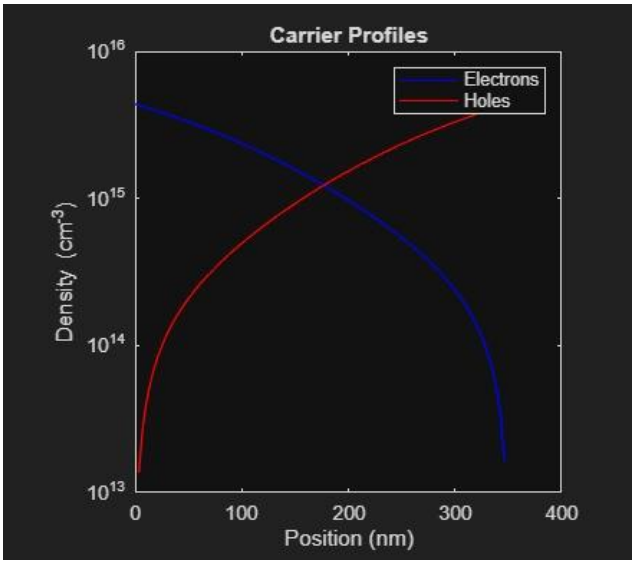

Figure 13: Carrier Profiles

In the case of lead-based materials, they do not give any electrical modeling results. This is one of the weaknesses of the comparative study. According to the established properties, carriers of perovskites including lead-based tend to have a higher mobility coupled with longer diffusion lengths and lower recombination. These characteristics allow an easy movement of charges and collection of the charges thus leading to performance improvement of the devices. The comparison of lead-free materials in terms of the detailed analysis of their electrical characteristics and the lack of these data in the case of the lead-based one demonstrate the gap in the comparison. Nevertheless, the low performance of the lead-free device in electrical terms evidently points to the necessity to generate a solution that would make sure that the limitations of materials and interfaces can be overcome in order to obtain a practically effective solution.

3.6 Current Density and Output Performance

The comparison of short-circuit current density of lead-based materials is provided in figure 14. As the figure demonstrates, $FAPbI_3$ attains the highest current density, which predetermines $MAPbI_3$ and $CsPbBr_3$. This is in line with their absorption and production nature. The increased current density of $FAPbI_3$ at high current density is attributed to the fact that this material can absorb a broader wavelength spectrum and can create more carriers.

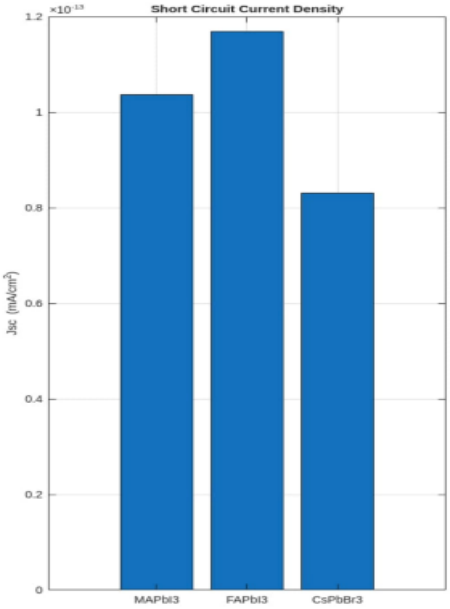

Figure 14: Jsc Comparison

On the contrary, the lead-free device presents an extremely low current density that is indicated in the J-V curve. This implies that there is a wide gap between the potential and the output in terms of output. Although the optical model is indicating good performance, the issue of electrical limitation does not allow efficient generation of current. In this comparison it is evident that the materials based on lead are better in converting the absorbed light to practicable electrical current, whereas the lead-free material is dominated by loss.

3.7 Overall Performance Comparison

As indicated in the table, simulated efficiency of $Cs_2AgBiBr_6$ is very high and it is about 21% when the conditions are optimized. Experimental values are however much lower usually ranging between 2-3%. This wide gap means that real effects like defects, recombination and interface losses all cause considerable performance loss. The materials based on tin are more efficient, but cannot be stabilized since they are oxidized. Materials based on bismuth-antimony are more resistant yet they are less efficient because of low carrier transport.

Table 1 reveals performance data of different lead-free perovskites materials.

Table 1: Experimental v. Simulated Performance

Material System	Device Structure	Efficiency (PCE, %)	Voc (V)	Jsc (mA/cm²)
$Cs_2AgBiBr_6$ (this work, simulated)	Glass/ ITO/ SnO_2/ $Cs_sAgBiBr_6$/ Spiro-OMeTAD/ Au	21% (optimal, 75 nm)	~0.8 (estimated)	~20
$Cs_2AgBiBr_6$ (experimental)	FTO/ TiO_2/ $Cs_2AgBiBr_6$/ Carbon	2.2%	0.72	4.5
$Cs_2AgBiBr_6$ (experimental, optimized)	Glass/ FTO/ TiO_2/ $Cs_2AgBiBr_6$/ Spiro/ Au	3.1%	0.84	6.0
$MASnI_3$ (Tin-based)	Glass/ FTO/ TiO_2/ $MASnI_3$/ Spiro/ Au	6–9%	0.6–0.7	18–22
$FA_3Bi_2I_9$ (Bismuth-based)	Glass/ FTO/ TiO_2/ $FA_3Bi_2I_9$/ Spiro/ Au	2–4%	0.9	5–8
$Cs_3Sb_2I_9$ (Antimony-based)	Glass/ FTO/ TiO_2/ $Cs_3Sb_2I_9$/ Spiro/ Au	3–6%	1.0	7–10

Compared to the lead-based materials of $MAPbI_3$ and $FAPbI_3$, which have demonstrated in the past a high level of optical performance as well as a high current generation, it is evident that the lead-based perovskites outcompete the lead-free variant in terms of effectiveness. Lead-based perovskites are very efficient and effective with respect to performance whereas the lead-free materials are much safer in terms of environment and stability without high practical efficiency. This is one of the gaps that the future research has to overcome.

4. DISCUSSION

This paper makes comparisons between lead-based and lead-free perovskite solar cells on the basis of optical and electrical analysis. The findings indicate a significant gap between the potentials and the performances in reality as far as lead-free materials are concerned. The lead-free perovskite is highly efficient to be simulated at the best thickness but the electrical performance is very poor. It implies that even in an ideal situation whereby the material is an efficient light absorber, it is unable to change that energy into useful electricity efficiently because of recombination losses as well as carrier transportation. There is strong optical performance of lead-based perovskites over a long wavelength. They are more light absorbing, produce more carriers and are denser. Although these materials do not have the electrical modeling, they have established properties that include a higher mobility and longer diffusion length which makes them better. This contributes towards the Lead based materials being more effective and dependable in actual devices.

The other notable aspect is stability and impact on the environment. Lead-free materials are more stable and safer and lack efficiency making their practical use limited. Lead-made materials are effective however they have challenges concerning toxicity and prolonged degradability. This gives a trade-off between performance and sustainability. The paper demonstrates that higher quality of materials, better defects, and interface are the three measures to enhance lead-free perovskites. Alternative to lead-based materials should also be developed, which are not hazardous. In the comparison, it is noted that research to be done in future must aim at integrating the benefits of the two systems in order to come up with a system that is highly efficient, stable and environmentally safe.

5. CONCLUSION

This paper involves the comparison of the lead-based and lead-free perovskite solar cells with respect to their efficiency, stability and operation. It is found that the lead-based materials are optimally absorbing in optical, respond in a broader spectrum, and generate more current. They are also capable of more in depth light penetration and even carrier generation is uniform.

Conversely, lead-free materials have severe weaknesses in electrically relevant characteristics of recombination loss and inefficient carrier transport. The lead-free perovskite is highly efficient in the simulation although the performance of the actual device is very low. This demonstrates that there is a wide difference between the theoretical and practical outcomes. Nevertheless, the materials that are lead-free are less reactive and less dangerous, so they are valuable in terms of the future development. The paper raises a trade-off between performance and sustainability. Ensuring enhancement of the material quality, minimizing defects, and carrier transportation in the lead-free perovskites should be improved in the future in order to justify their usage in real-life conditions.

REFERENCES

[1] Al Atem, M., and Y. Makableh, "Towards sustainable perovskite solar cells: Lead-free high efficiency designs with tin and germanium," *Eng*, vol. 6, no. 2, p. 38, 2025.

[2] B. W. Zhang *et al.*, "Lead-free perovskites and metal halides for resistive switching memory and artificial synapse," *Small Structures*, vol. 5, no. 6, p. 2300524, 2024.

[3] C. Ma *et al.*, "Light management in highly-textured perovskite solar cells: From full-device ellipsometry characterization to optical modelling for quantum efficiency optimization," *Solar Energy Materials and Solar Cells*, vol. 230, p. 111144, 2021.

[4] G. Haidari, "Comparative 1D optoelectrical simulation of the perovskite solar cell," *AIP Advances*, vol. 9, no. 8, 2019.

[5] H. Bencherif and M. K. Hossain, "Design and numerical investigation of efficient $(FAPbI_3)_{1-x}(CsSnI_3)_x$ perovskite solar cell with optimized performances," *Solar Energy*, vol. 248, pp. 137–148, 2022.

[6] K. A. Donkata, K. Beltako, M. M. Dzagli, and M. A. Mohou, "Numerical simulation and optimization of highly efficient inorganic lead-free perovskite solar cells using SCAPS-1D," *Scientific African*, p. e02841, 2025.

[7] M. N. Shaikh, Q. Zafar, and A. Papadakis, "A study of electromagnetic light propagation in a perovskite-based solar cell via a computational modelling approach," *Bulletin of Materials Science*, vol. 42, no. 4, p. 169, 2019.

[8] M. S. Salem, A. Shaker, M. M. Salah, M. El Sabbagh, and M. Gad, "Comprehensive TCAD simulation and optimization of lead-free $AgBiI_4$ solar cells: Migration from single cell to high-performance indoor photovoltaic modules," *Ain Shams Engineering Journal*, vol. 16, no. 5, p. 103371, 2025.

[9] M. Sulaman *et al.*, "Lead-free tin-based perovskite nanocrystals for high-performance self-driven bulk-heterojunction photodetectors," *Materials Today Physics*, vol. 27, p. 100829, 2022.

[10] M. T. Islam *et al.*, "Numerical simulation studies of a fully inorganic $Cs_2AgBiBr_6$ perovskite solar device," *Optical Materials*, vol. 105, p. 109957, 2020.

[11] O. D. Iakobson, O. L. Gribkova, A. R. Tameev, and J.-M. Nunzi, "A common optical approach to thickness optimization in polymer and perovskite solar cells," *Scientific Reports*, vol. 11, no. 1, p. 5005, 2021.

[12] O. O. Moyofola and M. E. Emetere, "Numerical analysis of the optoelectronic properties of selected Sn-based perovskite solar cells using SCAPS simulation," *Results in Optics*, vol. 21, p. 100868, 2025.

[13] S. Ali, P. Kumar, K. Ahmad, and R. A. Khan, "Simulation of lead-free perovskite solar cells with improved performance," *Crystals*, vol. 15, no. 2, p. 171, 2025.

[14] S. Beriha, A. Dikhit, and S. K. Tripathy, "Improving the efficiency of a FTO/PCBM/$Cs_2AgBiBr_6$/NiOx/Au lead-free double perovskite solar cell using numerical simulation through optimizing the absorption layer thickness and work function of electrodes," *Results in Optics*, vol. 12, p. 100467, 2023.

[15] S. Bhattarai, R. Pandey, J. Madan, D. Muchahary, and D. Gogoi, "A novel graded approach for improving the efficiency of lead-free perovskite solar cells," *Solar Energy*, vol. 244, pp. 255–263, 2022.

[16] S. H. Cheragee and M. J. Alam, "Device modeling and numerical study of a double absorber solar cell using a variety of electron transport materials," *Heliyon*, vol. 9, no. 7, 2023.

[17] S. H. Cheragee and M. J. Alam, "Device modelling and numerical analysis of high-efficiency double absorbers solar cells with diverse transport layer materials," *Results in Optics*, vol. 15, p. 100647, 2024.

[18] S. Haque *et al.*, "Photonic-structured perovskite solar cells: Detailed optoelectronic analysis," *ACS Photonics*, vol. 9, no. 7, pp. 2408–2421, 2022.

[19] S. Rahimi, M. Eskandari, and D. Fathi, "New nanostructure perovskite-based light-emitting diode with superior light extraction efficiency enhancement," *Scientific Reports*, vol. 14, no. 1, p. 5500, 2024.

[20] S.-S. Yan *et al.*, "Enhanced optoelectronic performance induced by ion migration in lead-free $CsCu_2I_3$ single-crystal microrods," *ACS Applied Materials & Interfaces*, vol. 14, no. 44, pp. 49975–49985, 2022.

FUNDING DECLARATION

This research did not receive any specific grant from funding agencies in the public, commercial, or not-for-profit sectors.

Sunaina